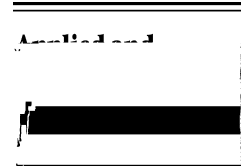




Appl. Comput. Harmon. Anal. 23 (2007) 235–253



www.elsevier.com/locate/acha

separated multiresolution representation for a class of convolution operators. These estimates provide the analytic foundation for accuracy control within the framework of separated representations of operators in high dimensions.

The kernels of operators of this class are non-oscillatory and include weakly singular and singular operators which are ubiquitous in problems of physics. The Poisson kernel and the projector on the divergence free functions provide two important examples with a wide range of applications in computational chemistry, computational electro-magnetics and fluid dynamics. However, these operators are rarely used directly for computing. For example, one typically solves the Poisson equation in the differential form as a step in solving the Navier–Stokes equations rather than apply the projector on ds

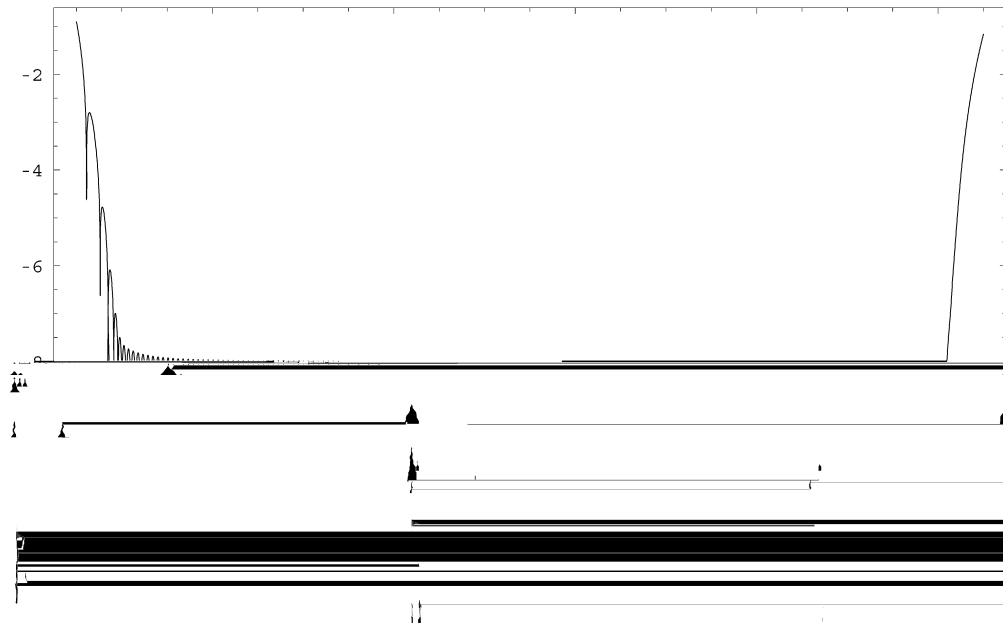


Fig. 1. Error (\log_{10}) of approximating the Poisson kernel using Proposition 1 with consequent optimization, where. $10^{-8}, 10^{-9} \leq x \leq 1$ and $M = 89$.

$$M = \log^{-1} [c_0 + c_1 \log^{-1} + c_2 \log \epsilon^{-1}], \tag{2}$$

$$c \dots F \dots M = \mathcal{O}(\log \epsilon^{-1}).$$

For singular operators, we will need a different measure of error in such approximations. Let us select. $= \epsilon^{-2}$ in Proposition 1 and arrive at

Proposition 2. $F > 0, 0 < \epsilon \leq 1, 0 < \dots \leq \min\{\frac{1}{2}, \frac{8}{\dots}\}, \dots$

$$\left| \dots - \sum_{n=1}^M e^{-n\epsilon} \right| \leq \dots \epsilon^{-2} \dots \epsilon \leq \dots \leq 1, \tag{3}$$

$$M = \log^{-1} [c_0 + c_1 \log^{-1} + c_2 \log \epsilon^{-1}]. \tag{4}$$

Propositions 1 and 2 provide an initial approximation that we optimized further to reduce the number of terms via the approach in [17]. The errors of such approximation are illustrated in Figs. 1 and 2.

We note that approximations of the function 1

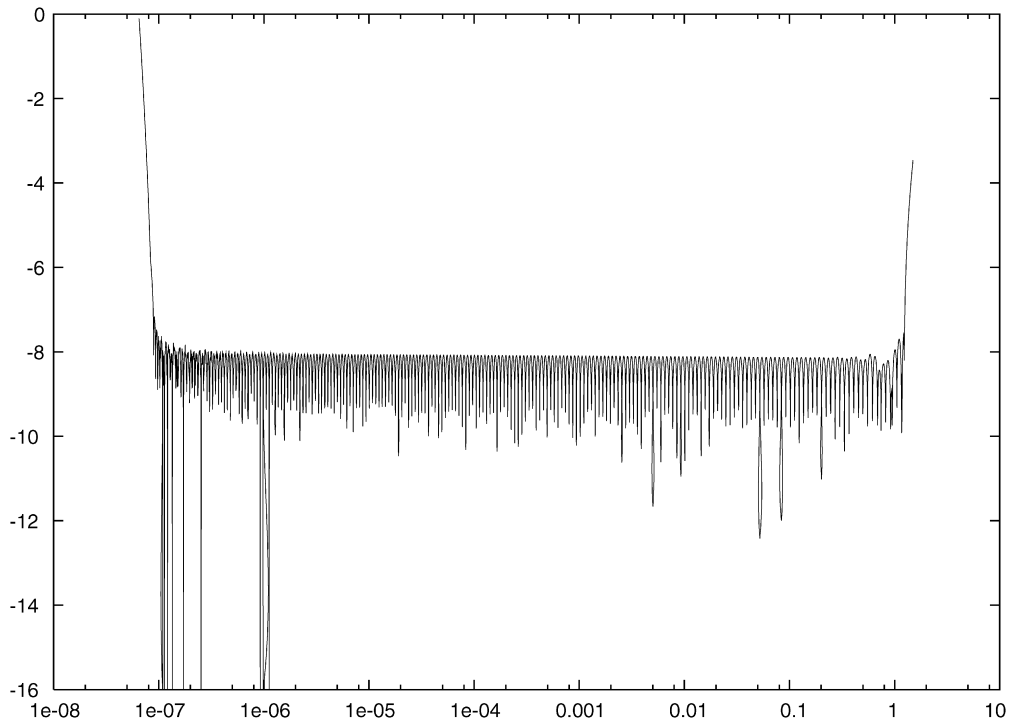


Fig. 2. Error (\log_{10}) of approximating $1/x^3$ using Proposition 2 with consequent optimization, where $10^{-8}, 10^{-7} \leq x \leq 1$ and $M = 110$.

by the trapezoidal rule, namely, setting $\rho_j = e^{2j}$ and $\Delta_j = 2\Delta e^{-j} / \Gamma(j/2)$, where $x_j = x_0 + (j-1)\Delta$, $j = 1, \dots, M$. For a given accuracy ϵ and range $0 < x_0 \leq x_M \leq 1$, we select x_0 and $x_M = x_0 + (M-1)\Delta$, the end points of

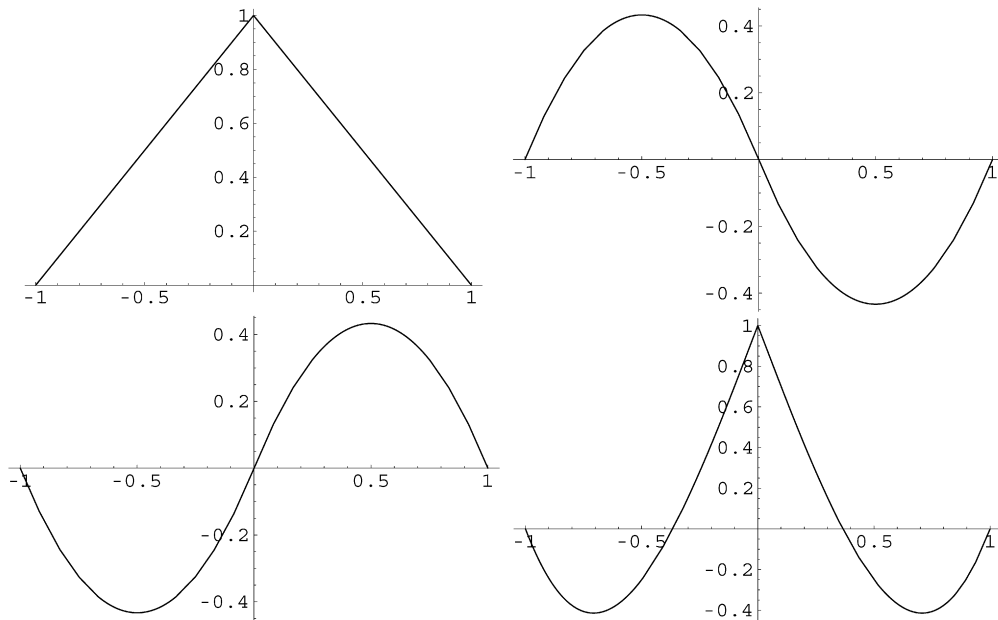


Fig. 3. The first four cross-correlation functions $i_0, i_1, i_2,$ and i_3 .

$$i_i(\tau) = \begin{cases} i_i^+(\tau), & 0 \leq \tau \leq 1, \\ i_i^-(\tau), & -1 \leq \tau < 0, \\ 0, & 1 < |\tau|, \end{cases} \tag{8}$$

where $i, i = 0, \dots, m - 1$ and

$$i_i^+(\tau) = \int_0^{1-\tau} i(\tau + \xi) i(\xi) d\xi, \quad i_i^-(\tau) = \int_{-\tau}^1 i(\tau + \xi) i(\xi) d\xi. \tag{9}$$

The first four cross-correlation functions are illustrated in Fig. 3.

We summarize relevant properties of the cross-correlation functions i_i in

- Proposition 3.** (1) $i_i(\tau) = (-1)^{i+i} i_i(\tau)$.
 (2) $i_i(-\tau) = (-1)^{i+i} i_i^+(\tau)$ $0 \leq \tau \leq 1$.
 (3) $i_i(0) = 0$ $i = i, i_i(0) = 1$ $i = 0, \dots, m - 1$.
 (4) $\max_{\tau \in [-1,1]} |i_i(\tau)| \leq 1$ $i, i = 0, \dots, m - 1$.
 (5) $C_{i+1}^{(-1/2)}(2 - 1) = \frac{1}{2} C_1^{(-1/2)}(2 - 1) + \frac{1}{2}$ $i_0(\tau) = \frac{1}{2} \sqrt{2i + 1} \times$
 (6) $C_{i+1}^{(-1/2)}(2 - 1) = \frac{1}{2} C_{i+1}^{(-1/2)}(2 - 1) + \frac{1}{2}$

$$b = \bar{3} + \mathbf{l} ,$$

$$F_{ii} = \int_{-1}^1 e^{-\mathbf{r}} ($$

$$G_{ii} = \frac{2}{b^2} \int_{-1}^1 e^{-\eta} (\eta + 1)^2 / b^2 (\eta + 1)^2 \eta_{ii}(\eta) d\eta - F_{ii} \quad (36)$$

(2) $\mathbf{l} = \mathbf{0} \quad i = i, j = j,$

If $\mathbf{l} = \mathbf{0}$ and $i = i, j = j$, and \dots , then for the off-diagonal terms we have

$$t_{ij}^{0,12} = \frac{1}{4} \int_B \frac{3 - |\mathbf{x}|^2}{|\mathbf{x}|^5} (i i - j j) (3) \, d\mathbf{x} = 0, \tag{55}$$

as the conditional limit of corresponding integrals for all i, j, \dots .

(4) If $\max_i |i| \geq 2$, then $\min_{B \setminus D} |\mathbf{x} + \mathbf{l}| = 1$ and the integral in (30) has no singularities. The estimate (44) is then obtained by using (49),

$$\left| t_{ij}^{\mathbf{l}} - t_{ij}^{\mathbf{l}} \right| \leq \frac{1}{4} \int_B \frac{d\mathbf{x}}{|\mathbf{x} + \mathbf{l}|^2} \leq \frac{1}{4} \frac{1}{3} \int_B \frac{d\mathbf{x}}{|\mathbf{x}|^2} = \dots \tag{56}$$

If $\max_i |i| \leq 1$, we split the domain of integration for $t_{ij}^{\mathbf{l}}$ into the neighborhood around the singularity $D, = \{\mathbf{x}: |\mathbf{x} + \mathbf{l}| \leq \epsilon\}$ and the rest of the domain, $B \setminus D$. The estimate for the integral over $B \setminus D$ is the same as in (56). We need, however, to estimate the integrals over D , for both the kernel and its approximation. Using $|i i| \leq 1$ and $|i i| \leq \tilde{C}$ for some constant \tilde{C} (except at zero), and changing variables to $\mathbf{y} = \mathbf{x} + \mathbf{l}$, we have for the diagonal term with $\dots = 1$,

$$\left| \frac{1}{4} \int_{D,} \dots \right|$$

using asymptotic expansions and, as a result, obtain for them simple analytic expressions. Moreover, if we combine the contributions of the terms with large exponents, we effectively remove the dependence on the parameter ϵ altogether. In the process of accounting for the singularity in this manner, we also reduce the separation rank of the representation. Although the separation rank is p

where $F_{ii}^+ = F_{ii}^- (\mu/b^2)$. The function $f_{ii}(\cdot)$ is a polynomial on subintervals $[0, 1]$ and $[-1, 0]$. Using the Taylor expansion in $[0, 1]$ at points $\xi = 0, 1$, we have

$$f_{ii}^+(\xi) = f_{ii}^+(\xi) + f_{ii}^+(\xi)(\xi - \xi) + f_{ii}^+(\xi) \frac{(\xi - \xi)^2}{2} + \dots, \tag{65}$$

where the one-sided derivatives are computed at the end points in directions from the interior of the interval $[0, 1]$ (outer derivative), and set $f_{ii}^+(\xi) = f_{ii}^+(\xi) = f_{ii}^+(\xi) = \dots = 0$ for all ξ outside $[0, 1]$. Similarly, we have expansion for $f_{ii}^-(\xi)$ in $[-1, 0]$ at points $\xi = -1, 0$,

$$f_{ii}^-(\xi) = f_{ii}^-(\xi) + f_{ii}^-(\xi)(\xi - \xi) + f_{ii}^-(\xi) \frac{(\xi - \xi)^2}{2} + \dots, \tag{66}$$

and set $f_{ii}^-(\xi) = f_{ii}^-(\xi) = f_{ii}^-(\xi) = \dots = 0$ for all ξ outside $[-1, 0]$.

For large μ (say, $\mu > 100$), we replace $e^{-\mu}$, $\text{erf}(\mu)$ and $\text{erf}(-\mu)$ by their limits. Here $\text{erf}(\cdot)$ denotes the error function,

$$\text{erf}(\xi) = \frac{2}{\sqrt{\pi}} \int_0^\xi e^{-t^2} dt. \tag{67}$$

Since $\text{erf}(-\xi) = -\text{erf}(\xi)$, $\text{erf}(0) = 0$ and $\text{erf}(\mu) \approx 1$ for large μ , we have for $\xi = 0, 1$,

$$\int_0^1 e^{-\mu(\xi - \xi)^2} d\xi = \frac{1}{\sqrt{\mu}} [\text{erf}(\mu) - \text{erf}((\xi - \xi)\mu)] / 2\mu^{1/2} \approx \frac{1}{\sqrt{\mu}} / 2\mu^{1/2},$$

$$\int_0^1$$

$$F_{ii, jj} = 3 \frac{ii^+(-1) + ii^-(-1)}{2} \frac{jj^+(-2) + jj^-(-2)}{2} (-3) + \mathcal{O}(e^{-3(M_0)}). \quad (78)$$

Proof. In this case we need to estimate for large ρ the contribution from (36). Introducing

$$G_{ii}(\rho) = S_{ii}(\rho) - F_{ii}(\rho) \quad (79)$$

with

$$S_{ii}(\rho) = 2\rho \int_{-1}^1 e^{-\rho(x-1)^2} (x-1)^2 ii(x) dx, \quad (80)$$

we have $G_{ii} = G_{ii}^- (\rho/b^2)$. Using (68) and (69), as well as

$$T_{ii}(\rho) = \int_{-1}^1 (x-1)^3 e^{-\rho(x-1)^2} dx \quad \begin{cases} 1, \Delta \Gamma \Gamma TD (\Delta Tj / F \Delta S \Delta e) \\ \Gamma TD \Gamma \end{cases}$$

If $l = 0$ then the additional term is obtained from (75) by setting indices to zero and evaluating the cross-correlation functions explicitly.

For computing the off-diagonal terms, we need to estimate for large ρ

$$T_{ii}(\rho) = \int_{-1}^1 e^{-\rho(x-)^2} (x-)^{ii} dx. \quad (87)$$

Using (68) and (69), and observing that $ii(\pm 1) = 0$, we obtain for $\rho = -1, 0, 1$

$$T_{ii}(\rho) = -\frac{ii^+ + ii^-}{4\rho^3}$$

Introducing the orthogonal projector on V_j , $P_j : L^2(\mathbb{R}^d) \rightarrow V_j$ and considering an operator $T : L^2(\mathbb{R}^d) \rightarrow L^2(\mathbb{R}^d)$, we define its projection $T_j : V_j \rightarrow V_j$ as $T_j = P_j T P_j$. This projection is written explicitly in (13) in dimension $d = 3$ for convolution operators with the kernel $K(\mathbf{x} - \mathbf{y})$.

We also consider the orthogonal projector $Q_j : L^2(\mathbb{R}^d) \rightarrow W_j$, defined as $Q_j = P_{j+1} - P_j$. The non-standard form of the operator T is the collection of components of the telescopic expansion

$$T_j = (T_j - T_{j-1}) + (T_{j-1} - T_{j-2}) + \dots + T_0 = T_0 + \sum_{j=0}^{j-1} (A_j + B_j + C_j),$$

where $A_j = Q_j T Q_j$, $B_j = Q_j T P_j$, and $C_j = P_j T Q_j$. The main property of this telescopic expansion is that the rate of decay of the matrix elements of operators A_j , B_j , and C_j away from the diagonal is controlled by the number of vanishing moments of the basis and, for a finite but arbitrary accuracy, the matrix elements outside a certain band can be set to zero resulting in an error of the norm less than ϵ . Such behavior of the matrix elements becomes clear if we observe that the derivatives of the kernels under consideration decay faster than the kernel itself and, in our case, the rate of decay corresponds to the number of derivatives taken. If we use the Taylor expansion of the kernel to estimate the matrix elements away from the diagonal, then the size of these elements is controlled by a high derivative of the kernel since the vanishing moments remove the lower order terms [1].

Applying the non-standard form to a function, we write

$$T_j f = T_0 f + \sum_{j=0}^{j-1} (A_j(Q_j f) + B_j(P_j f) + C_j(Q_j f)), \tag{90}$$

where the operators P_j and Q_j are inserted to indicate the necessary projections of the function f . The advantage of the non-standard form is that it accounts for the interaction between different scales via an operator-independent projection applied after evaluating all of the components in (90). Namely, we observe that although the components $A_j f + C_j f \in W_j$, are a part of the multiwavelet expansion, the components $B_j f \in V_j$ need to be projected on the appropriate wavelet subspaces [1] to obtain the final result.

We note that there are several ways to implement the application of the non-standard form to functions. Using Theorems 9 and 10, a new adaptive algorithm has been developed recently and will be described elsewhere [16].

7. Conclusions

Using the Poisson kernel and the projector on the divergence free function as examples, we have constructed separated representations of these kernels in multiwavelet bases. A similar approach is applicable to non-homogeneous convolutions, for example kernels $e^{-\gamma \|\mathbf{x}\|} / \|\mathbf{x}\|$, where $\gamma > 0$ and $\mathbf{x} \in \mathbb{R}^3$, used in [4] and [5]. The key to these computations are separated approximations described in Section 2.1. Our approach also reveals the structure of operators on fine scales depicted in Theorems 9 and 10.

Appendix A

Let us provide a brief proof of properties of the cross-correlation functions in Proposition 3.

(1) Since $P_i(-\mathbf{x}) = (-1)^i P_i(\mathbf{x})$, we have from (6) $i(-\mathbf{x} + 1) = (-1)^i i(\mathbf{x})$. Setting $\mathbf{x} + 1 = -\mathbf{x} + 1$ in (7), we obtain

$$ii(\mathbf{x}) = \int_{-\infty}^{\infty} i(-\mathbf{x} + 1) i(-\mathbf{x} - 1) d\mathbf{x} = (-1)^{i+i} \int_{-\infty}^{\infty} i(\mathbf{x}) i(\mathbf{x} + 1) d\mathbf{x}.$$

(2) The relations between i^+ and i^- follow from the direct examination of (8) and (9).

(3) Since

$$ii^+(0) = \int_0^1 i(\mathbf{x} + 1) i(\mathbf{x}) d\mathbf{x},$$

the values at zero are obtained using the orthonormality of the scaling functions ϕ_i .

(4) Let us obtain the upper bound for $\sum_{i=0}^n \phi_i^2$ using (9). We have

$$\int_0^{1-} \left| \sum_{i=0}^n \phi_i(x) \right|^2 dx$$

[11] G. Beylkin, Approximations and fast algorithms, in: A. Laine, M. Unser, A. Aldroubi (Eds.), *Wavelets: Applications in Signal and Image*